Title

Inhibition of WNT signaling attenuates self-renewal of SHH-subgroup medulloblastoma

Journal

Oncogene, 36(45)

ISSN

0950-9232

Authors

Rodriguez-Blanco, J

Pednekar, L

Penas, C

et al.

Publication Date

2017-11-09

DOI

10.1038/onc.2017.232

Peer reviewed

HHS Public Access

Author manuscript

Oncogene. Author manuscript; available in PMC 2017 November 10.

Published in final edited form as:

Oncogene. 2017 November 09; 36(45): 6306–6314. doi:10.1038/onc.2017.232.

Inhibition of WNT signaling attenuates self-renewal of SHH-subgroup medulloblastoma

J Rodriguez-Blanco[1], **L Pednekar**[1], **C Penas**[2], **B Li**[1], **V Martin**[3], **J Long**[1], **E Lee**[4], **WA Weiss**[5], **C Rodriguez**[3], **N Mehrdad**[6], **DM Nguyen**[7,8], **NG Ayad**[2,8], **P Rai**[8,9], **AJ Capobianco**[1,8], and **DJ Robbins**[1,8]

[1]Molecular Oncology Program, The DeWitt Daughtry Family Department of Surgery, University of Miami, Miller School of Medicine, Miami, FL, USA

[2]Center for Therapeutic Innovation, Department of Psychiatry and Behavioral Sciences, University of Miami, Miller School of Medicine, Miami, FL, USA

[3]Morphology and Cell Biology Department, University of Oviedo, Asturias, Spain

[4]Department of Cell and Developmental Biology, Vanderbilt University, Nashville, TN, USA

[5]Department of Neurobiology, University of California, San Francisco, CA, USA

[6]Department of Pathology, University of Miami, Miller School of Medicine, Miami, FL, USA

[7]Division of Cardiothoracic Surgery, The DeWitt Daughtry Family Department of Surgery, University of Miami, Miller School of Medicine, Miami, FL, USA

[8]Sylvester Comprehensive Cancer Center, University of Miami, Miami, FL, USA

[9]Department of Medicine, University of Miami, Miller School of Medicine, Miami, FL, USA

Abstract

The SMOOTHENED inhibitor vismodegib is FDA approved for advanced basal cell carcinoma (BCC), and shows promise in clinical trials for SONIC HEDGEHOG (SHH)-subgroup medulloblastoma (MB) patients. Clinical experience with BCC patients shows that continuous exposure to vismodegib is necessary to prevent tumor recurrence, suggesting the existence of a vismodegib-resistant reservoir of tumor-propagating cells. We isolated such tumor-propagating cells from a mouse model of SHH-subgroup MB and grew them as sphere cultures. These cultures were enriched for the MB progenitor marker SOX2 and formed tumors *in vivo*. Moreover, while their ability to self-renew was resistant to SHH inhibitors, as has been previously suggested, this self-renewal was instead WNT-dependent. We show here that loss of *Trp53* activates canonical

Correspondence: Dr DJ Robbins, Molecular Oncology Program, The DeWitt Daughtry Family Department of Surgery, University of Miami Miller School of Medicine, 1600 NW 10th Avenue, Miami, FL 33136, USA. drobbins@miami.edu.

CONFLICT OF INTEREST

The authors declare no conflict of interest.

AUTHOR CONTRIBUTIONS

DJR and JR-B conceived and designed the experiments. JR-B performed the experiments. LP, CP and BL contributed to mouse work. JR-B and DJR analyzed the data. JL and EL contributed reagents/materials/analytic tools. VM, CR, DMN, PR, EL, WAW and AJC gave technical support and conceptual advice. NM provided pathological insights. DJR and JR-B wrote the paper.

Supplementary Information accompanies this paper on the Oncogene website (http://www.nature.com/onc)

WNT signaling in these SOX2-enriched cultures. Importantly, a small molecule WNT inhibitor was able to reduce the propagation and growth of SHH-subgroup MB *in vivo*, in an on-target manner, leading to increased survival. Our results imply that the tumor-propagating cells driving the growth of bulk SHH-dependent MB are themselves WNT dependent. Further, our data suggest combination therapy with WNT and SHH inhibitors as a therapeutic strategy in patients with SHH-subgroup MB, in order to decrease the tumor recurrence commonly observed in patients treated with vismodegib.

INTRODUCTION

Medulloblastoma (MB) is the most common malignant brain tumor of childhood.[1] While the bulk of patients respond to multimodal therapy (surgery, radiation and cytotoxic chemotherapy), treatment-induced morbidity leaves survivors with significant neurocognitive and endocrine disabilities.[2] These patients thus require therapies that promise to be more effective and less toxic. The classification of MB into four molecular subgroups[3,4] provided a template with which to begin identifying and testing such targeted therapies.[5,6] The best characterized subgroup is driven by the SONIC HEDGEHOG (SHH) signaling pathway, most commonly via mutation and loss of the gene encoding the SHH receptor PATCHED (PTCH). The SHH inhibitor vismodegib targets the upstream signaling component SMOOTHENED (SMO) and is FDA-approved for advanced basal cell carcinoma,[7] which is almost uniformly driven by SHH signaling.[8,9] As similar SMO inhibitors effectively target SHH-dependent mouse models of MB, significantly reducing the bulk of such tumors,[10] they are now being tested in SHH-subgroup MB patients.[11–13]

Tumors are heterogeneous, comprised of immune, stromal and tumor cells proper. Even the tumor cells themselves show significant variation in morphologies, proliferation rates and self-renewing capacity.[14,15] This heterogeneity is thought to result from a hierarchical organization, in which a small population of relatively quiescent, long-lived, multipotent, propagating/initiating cells drives the production of a population of rapidly amplifying progenitor cells, which in turn can give rise to more differentiated cell types.[16] Although the progenitor cells constitute the bulk of the tumor, they have limited self-renewing capacity, and are thus maintained by the smaller population of tumor-propagating cells. The tumor-propagating cells are relatively chemotherapy resistant, and are therefore thought to drive the tumor recurrence often observed in patients treated with chemotherapy.[17] Similarly, while limited clinical experience with SMO inhibitors in clinical trials has shown that there is often a rapid initial response to vismodegib, this is frequently followed by aggressive recurrent MB growth.[11,18] Additionally, it was noted that basal cell carcinoma patients often exhibited rapid recurrence upon vismodegib cessation, consistent with such tumors harboring a reservoir of vismodegib-resistant cells capable of driving recurrence.[19–22]

A number of tumor-propagating cells have been described for the SHH-subgroup of MB, with distinct properties, biomarkers, sensitivity to SMO inhibitors and abilities to be propagated as neurospheres *ex vivo*.[23–28] Most recently, lineage tracing in a mouse model of SHH MB identified a small population of $SOX2^+$ MB propagating cells (MPCs), and a population of $SOX2^-$ cells that constituted the bulk of the tumor proper.[28,29] The $SOX2^+$

cells were capable of efficient self-renewal but resistant to vismodegib, while the $SOX2^{-}$ cells exhibited a more limited capacity for self-renewal but were sensitive to vismodegib. Consistent with this observation, treatment of this mouse model of MB with vismodegib led to an enrichment of $SOX2^{+}$ cells in the residual tumor.[28] These $SOX2^{+}$ cells may contribute to recurrence observed in patients treated with vismodegib. Here, we show that self-renewal of $SOX2^{+}$ enriched sphere cultures (SCs) is dependent on canonical WNT activity, and that loss of *Trp53* drives this WNT dependence. A small molecule WNT inhibitor also depleted this population of $SOX2^{+}$ cells in SHH-subgroup MB *in vivo*, significantly reducing the ability of SHH tumors to propagate.

RESULTS

Characterization of MB sphere cultures

SHH-subgroup MBs harbor a small and phenotypically primitive population of MPCs that are enriched in cultured neurospheres *ex vivo*.[25,27] We isolated and characterized the MPC-like characteristics of three independent $Ptch1^{-/-}$-;$Trp53^{-/-}$ neurosphere cultures (SC 1–3). These cultures were enriched for neural stem cell markers, such as *Nestin* and *Sox2*, relative to bulk MB tissue (Figure 1a). They also displayed the cellular heterogeneity previously described for MPCs enriched cultures,[25,30] as evidenced by the mutually exclusive staining of a neural stem cell marker (NESTIN) with that of a neuronal progenitor marker (β3-TUBULIN) (Figure 1b). The SCs could be induced to express biomarkers of three distinct neural lineages (Figure 1c), suggesting that they are also pluripotent. Consistent with them being enriched for tumor-propagating cells, as few as 5000 SC cells were able to form tumors when implanted into mice (Figure 1d). SOX2 has previously being described as a biomarker for such tumor-propagating cells.[28,29] We therefore quantitated the percentage of $SOX2^{+}$ cells in the SCs relative to that in primary MB tissue. $SOX2^{+}$ cells were considerably more enriched in the SCs, relative to the approximate 5% of such cells observed in primary MB (Figure 1e).

The self-renewal of MPCs is dependent on WNT activity

The MPC enriched SCs were exposed to the SMO inhibitors cyclopamine and vismodegib, the inactive cyclopamine analog tomatidine, or a vehicle control. Interestingly, even though the parental MB tissue responded to vismodegib *in vivo* (Supplementary Figure S1A), neither SMO inhibitor had significant effects on the cellular viability (Supplementary Figures S1B,C) or self-renewal (Supplementary Figures S1D,E) of the three SCs. However, they both attenuated SHH target gene expression (Supplementary Figures S1F,G,H) relative to either a vehicle control or cultures treated with tomatidine. These results suggest that SMO inhibitors are capable of attenuating SHH signaling, but that such attenuation has only minimal biological affects in these *Trp53*-deficient SCs.

A WNT-driven gene expression profile was previously observed in $Ptch1^{+/-}$;$Trp53^{-/-}$ SCs.[27] Further, SOX2 expression, for which the SCs are enriched (Figure 1e), is WNT-dependent in many physiological settings.[31] Thus, we hypothesized that the MB SCs we had isolated were WNT-dependent. Consistent with this hypothesis, SCs were enriched for WNT signaling biomarkers relative to primary MB (Figure 2a). To directly test whether SCs are WNT-

dependent we transfected them with pools of siRNA targeting the pivotal WNT signaling component *β-Catenin* (*Ctnnb1*), green fluorescent protein (GFP), or a scrambled control siRNA. Relative to the control siRNAs, the *Ctnnb1* siRNA reduced the expression of the WNT biomarker *Lgr5* as well as *Sox2*, but had no effect on the SHH target genes *Gli1* or *Ptch2* (Figure 2b). Further, the *Ctnnb1* siRNA attenuated the self-renewal capability of the SCs (Figure 2c), but had little effect on the overall viability of these cultures (Supplementary Figure S2A). Although WNT activation in MB is commonly linked to *Ctnnb1* mutations,[32,33] no *Ctnnb1* mutations were identified in the SCs (Supplementary Figure S2B). As β-CATENIN also plays an essential role in E-CADHERIN signaling, distinct from its role in WNT signaling,[34] we also utilized a dominant negative form of the WNT transcription factor TCF3 (*dnTCF3*) commonly used to definitively identify WNT-dependent biomarkers.[35] Cultures expressing *dnTCF3* exhibited significantly attenuated WNT target gene expression, including *Sox2*, but had no effect on the expression of two SHH target genes (Figure 2d). SCs expressing *dnTCF3* had a reduced capacity for self-renewal (Figure 2e), but exhibited no change in viability (Figure 2f). To examine if the WNT activation we observe in SCs is ligand-driven we overexpressed a negative regulator of the canonical WNT pathway, *DKK1*, which antagonizes the LRP5/6 WNT co-receptor.[36] Overexpression of *DKK1* downregulated WNT target gene expression (Figure 2g), and reduced secondary sphere formation (Figure 2h) without affecting cell viability (Figure 2i). Combined, these results suggest that WNT signaling plays an important role in the self-renewal of the SCs, but a more minimal role in the immediate viability of these cultures. Consistent with this suggestion, two small-molecule activators of WNT signaling (GSK-3β inhibitors)[37] significantly increased the self-renewal capacity of these SCs (Supplementary Figure S2C).

Small-molecule WNT inhibitors attenuate the self-renewal of MPCs To identify a small-molecule WNT inhibitor that could be used to attenuate MB growth *in vivo*, we screened a number of mechanistically distinct small-molecule WNT inhibitors for their ability to attenuate self-renewal *ex vivo*. As downregulation of WNT signaling by *DKK1* overexpression reduced secondary sphere formation (Figure 2h), and DKK1 acts to suppress ligand-dependent WNT signaling,[36] we tested a small-molecule that directly attenuates WNT ligand activity, the PORCUPINE inhibitor LGK974.[38] Similar to *DKK1* overexpression, PORCUPINE inhibition reduced WNT pathway activation (Figure 3a) and secondary sphere formation (Figure 3b), without affecting SC viability (Figure 3c). Consistent with this WNT activation being ligand driven, *Wnt7a* and *Wnt7b* were highly expressed in SCs relative to parental MB tissue (Supplementary Figure S3A).

As both *Ctnnb1* knockdown (Figure 2c) and overexpression of *dnTCF* reduced secondary sphere formation (Figure 2e), we included in our screening antagonists of the TCF/β-CATENIN complex: carnosate,[39] CCT-031374,[40] ICG-001[41] and PKF115-584.[42] We first confirmed that this panel of TCF/β-CATENIN antagonists reduced WNT activity in a WNT-dependent reporter assay (Supplementary Figure S3B). We next treated SCs with these antagonists and observed a significant reduction in secondary sphere formation (Figure 3d), which occurred at lower doses than those that had effects on SC viability (Figure 3e). These WNT inhibitors also attenuated the expression of WNT target genes in SCs (Figure 3f), consistent with an on-target mechanism of action. We also verified that one of these inhibitors, carnosate, reduced the expression of *Sox2* (Supplementary Figure S3C) and the

numbers of $SOX2^+$ cells in these cultures (Supplementary Figure S3D). Finally, we determined if carnosate affects either proliferation or survival of SOX^+ cells. No changes in the expression of either proliferation proliferating cell nuclear antigen (PCNA) or apoptotic (CLEAVED CASPASE-3) biomarkers were observed in $SOX2^+$ cells (Supplementary Figure S3E), consistent with minimal changes in the number of viable cells in culture after longer exposure to WNT inhibitor (Supplementary Figure S3F). Together, these results are consistent with WNT signaling controlling *Sox2* expression, which is required for SCs to self-renew.

Loss of *Trp53* results in WNT-dependent self-renewal

A number of groups have previously shown that WNT activation attenuates SHH-subgroup MB growth,[43–45] observations inconsistent with our results. These previous results were obtained using *SmoA1*- or *Ptch1*-driven MB mouse models, or cells derived from such mice, which in all cases were in a wild type (WT) *Trp53* background. Thus, we hypothesized that the WNT requirement for SC self-renewal that we observe results from loss of *Trp53*. To test this hypothesis, we compared the expression of WNT biomarkers in $Ptch1^{-/-}$ SCs expressing WT *Trp53* or deficient for *Trp53*. We noted that expression of WNT biomarkers, including WNT ligands, was significantly reduced in the SCs expressing WT *Trp53* (Figure 4a). SCs expressing WT *Trp53* were unresponsive to small-molecule β-CATENIN/TCF inhibitors, as carnosate was unable to downregulate the expression of WNT target genes (Figure 4b), attenuate self-renewal (Figure 4c) or affect viability (Figure 4d). Further, overexpression of *dnTCF3* did not attenuate WNT target gene expression (Figure 4e) or self-renewal (Figure 4f) in WT *Trp53* SCs, but did in *Trp53*-deficient cultures. The cell viability of either SC was not reduced by *dnTCF3* (Supplementary Figure S4A). To more directly address the effects of P53 on WNT signaling we attenuated P53 activity in SCs expressing WT *Trp53* and expressed WT *Trp53* in those cultures deficient in *Trp53*, and determined P53 and WNT activity. We observed increased expression of a P53 target gene (*Mdm2*) and decreased expression of WNT target genes upon transfection of $Ptch1^{-/-}$ *SCs* deficient in *Trp53* with a plasmid expressing WT *Trp53* (Figure 4g). Conversely, reducing P53 activity in $Ptch1^{-/-}$ *SCs* WT for *Trp53*, via expression of a dominant negative *Trp53* construct or treatment with the small-molecule P53 inhibitor [Pifithrin-α (PFTα)], reduced *Mdm2* expression but increased expression of WNT target genes (Figures 4h and i). Together, these results suggest that loss of *Trp53* results in increased WNT activity in *Ptch1* mutation-driven SCs.

MB growth and propagation is WNT-dependent

To examine the dependence of MB growth and initiation on WNT signaling *in vivo*, we implanted *Trp53* mutant, *Ptch1*-driven MB tissue, which had never been cultured *ex vivo*, into the brains of immunocompromised mice and treated them with vehicle or carnosate. Carnosate was selected for these *in vivo* studies based on *ex vivo* efficacy and its blood brain barrier penetrance.[46] These mice were treated for 20 days, or until they displayed behavior consistent with having MB (head tilt, hunched posture, ataxia, weight loss), at which time the mice were killed and their brains collected for further analyses. We noted that orthotopically grown MBs were significantly smaller in carnosate treated mice relative to vehicle treated mice (Figures 5a and b). These smaller residual tumors had decreased

numbers of proliferating cells, as determined by PCNA immunostaining (Figure 5c, Supplementary Figure S5A), and decreased numbers of $SOX2^+$ cells (Figure 5d, Supplementary Figure S5B). These results appear distinct from our *ex vivo* experiments in which carnosate did not affect culture growth (Figure 3e, Supplementary Figure S3F). We speculate that the effects we see on MB cell proliferation *in vivo* are indirect, resulting from loss of the MPCs that drive bulk tumor growth. Likely, similar effects were not observed *ex vivo* because of the significantly reduced time such cultures were exposed to carnosate.

To determine the WNT dependence of MPCs *in vivo*, we implanted MB tissue into the flanks of mice and treated them with carnosate or vehicle once tumor growth was palpable. Carnosate significantly reduced the expression of WNT target genes, but not SHH target genes, in these tumors (Figure 5e), and reduced the numbers of $SOX2^+$ cells (Figure 5f, Supplementary Figure S5C). Consistent with carnosate treatment reducing the number of MPCs, MB tissue from the carnosate-treated primary tumors also displayed significantly reduced ability to initiate new tumors when similar numbers of viable donor cells were reimplanted into recipient mice (Figure 5g). We also reimplanted carnosate-treated MB tissue from donor mice orthotopically into naïve recipient mice, and monitored their MB symptom-free survival. Consistent with carnosate treatment reducing MB propagation, mice harboring carnosate-treated tumor tissue exhibited significantly increased MB symptom-free survival over those that received MB tissue from vehicle-treated donors (Figure 5h).

DISCUSSION

The WNT signaling pathway regulates multiple aspects of stem cell function. Indeed, WNT ligands play key roles in neuronal stem cell self-renewal,[31] symmetric division,[47] pluripotency[48] and tumor initiation in cancer stem cells.[31,49] We show here that the self-renewal of multipotent, $SOX2^+$-enriched SCs, which ultimately drive the growth of *Trp53*-deficient SHH-subgroup MB, is dependent on WNT activity. This conclusion is based on inhibiting several components of the canonical WNT signaling pathway, using both molecular genetic and small-molecule inhibitors (Supplementary Figure S6). Further, we show that a small-molecule WNT inhibitor is able to reduce the number of $SOX2^+$ cells, tumor initiation and tumor growth *in vivo*, increasing the overall survival of mice harboring *Trp53*-deficient SHH-subgroup MB.

Our *Trp53*-deficient SCs had reduced expression of SHH biomarkers relative to primary MB tissue, which is likely why they were resistant to SMO inhibitors.[50] However, these cultures expressed both WNT ligands and biomarkers associated with an activated WNT signaling pathway. Consistent with MPC self-renewal being WNT ligand-dependent, a PORCUPINE inhibitor, which reduces WNT ligand activity,[38] or overexpression of *DKK1*, which attenuates WNT co-receptor activation,[36] prevented SCs self-renewal. The self-renewal of *Trp53*-deficient SCs also required canonical β-CATENIN/TCF activity, as knockdown of *β-Catenin*, overexpression of *dnTCF3*, or four distinct small-molecule inhibitors of this WNT-dependent transcriptional complex, inhibited self-renewal. Based on the sensitivity of these cultures to these mechanistically distinct small molecule and molecular genetic regulators of WNT signaling, we suggest that the MPC-enriched cultures elaborate a WNT ligand-

dependent activation of canonical β-CATENIN/TCF signaling, which ultimately drives SC self-renewal.

It was previously suggested that WNT signaling attenuates the growth of SHH-subgroup MB.[43–45] This work showed that the repressive effect of WNT activity on SHH-subgroup MB was indirect, via downregulation of SHH signaling. The major difference between these previous studies and our work is that we use a *Trp53*-deficient mouse model of MB. Consistent with this previous work, we show that SCs expressing WT *Trp53* do not express high levels of WNT biomarkers, are not sensitive to WNT inhibition and do not self-renew in a WNT-dependent manner. However, we also show that reducing P53 activity in these WT *Trp53* cultures increased WNT activity and that overexpression of *Trp53* in *Ptch1*$^{-/-}$;*Trp53*$^{-/-}$ SCs reduced WNT activity. Together, these results suggest that loss of *Trp53* expression modulates the WNT dependence of *Ptch1* mutant-driven MB. Similarly, it was previously suggested that P53 can repress canonical WNT signaling in several tumor types. In some tumors, such as neuroblastoma and breast cancer, this regulation was shown to occur via the transcriptional activation of specific micro-RNAs.[51,52] While in colorectal cancer, loss of *TRP53* activates WNT signaling via BONE MORPHOGENIC PROTEIN signaling.[53]

TRP53 status is the most important risk factor of SHH-subgroup MB patients.[13,54,55] These patients, who tend to be children with germline *TRP53* mutations, exhibit a significantly reduced 5-year survival rate.[56] Further, clinical trials of vismodegib noted reduced progression-free survival of SHH-subgroup MB patients deficient in P53 activity.[13] Our findings suggest a model in which loss of *Trp53* results in the emergence of a vismodegib resistant, WNT-dependent population of MPCs. We further suggest that this population of WNT-dependent MPCs might underlie the poor outcome and relative vismodegib resistance of SHH-subgroup patients deficient in *TRP53*. Indeed, a similar model in which WNT-dependent basal cell carcinoma propagating cells drive bulk SHH-dependent basal cell carcinoma growth has been described.[57,58] Although the translational relevance of our findings using mouse models of MB are not yet known, we speculate that a therapeutic approach using WNT inhibitors would improve the outcome of *TRP53*-deficient SHH-subgroup patients. Importantly, such patients would likely benefit most from the use of combination therapy that also includes conventional chemotherapy or one of the SMO inhibitors now in clinical trials. Such a therapeutic strategy would inhibit the growth of the bulk tumor by targeting the rapidly dividing MB cells as well as target the MPCs that are resistant to such agents.[59]

MATERIALS AND METHODS

MPC enrichment and assay

MB tissue was enzymatically and mechanically digested using the Papain Dissociation System (Worthington, Lakewood, NJ, USA).[60,61] The resulting cell suspensions were grown *ex vivo* in Neurobasal serum-free medium containing 1% Glutamax, 2% B27, 1% N2, epidermal growth factor (25 ng/ml), fibroblast growth factor (25 ng/ml) and Pen-Strep (Invitrogen, Frederick, MD, USA) and allow to form spheres for up to 10 days. For analysis by immunocytochemistry, SCs were plated on poly-L-lysine-coated glass chamber slides

(Millipore, Billerica, MA, USA) in the medium described above or in Neurobasal medium containing 2% fetal bovine serum for 6 days, essentially as previously described.[62] All primary antibodies including: SOX2 #ab97959 (Abcam, Cambridge, UK), PCNA #2586, GFAP #12389, CNPASE #5664, β3-TUBULIN #5568, NESTIN #4760, NEUROFILAMENT-L #2837 (Cell Signaling, Danvers, MA, USA) were used according to their manufacturer's instructions. For analyses by flow cytometry, cell suspensions from SCs or tumor tissues were incubated in Cytofix/Cytoperm solution (Becton & Dickinson, Franklin Lakes, NJ, USA) prior to staining with the corresponding fluorescent-conjugated antibody: SOX2 #656103, PCNA #307909 (BioLegend, San Diego, CA, USA), and CLEAVED CASPASE-3 #9669 (Cell Signaling). Fluorescence activated cell sorting (FACS) data were acquired using a BD CANTO II FACS (Becton & Dickinson) and analyzed using DiVa6 software.

Cell and molecular biology

Plasmids expressing a dominant-negative *TCF3* construct (*dnTCF3*),[63] *DKK1* (Addgene, Cambridge, CA, USA), *Trp53* (Takara, Mountain View, CA, USA), a dominant-negative P53 (*dnTrp53*) (Takara) or siRNA smart pools (Dharmacon, Lafayette, LA, USA) were transfected into SCs using Lipofectamine 2000 (Invitrogen). Cell viability was monitored by the reduction of 3-(4,5-dimethyl-2-thiazolyl) 2,5-diphenyl-2H-tetrazolium bromide to formazan,[64] or by trypan blue exclusion when evaluating the number of viable cells prior to sphere formation assays, FACS analysis or engraftment *in vivo*. Secondary sphere formation was determined using equal numbers of viable cells, from treated primary SCs, to form spheres in 8 days. Total RNA was Trizol (Invitrogen) extracted and the expression of the indicated genes determined using quantitative real-time PCR (RT–qPCR) and Taqman probes (Invitrogen), followed by normalization to the expression of *Gapdh*.[65] The efficacy of WNT antagonists was validated using a mycoplasma tested cell line and containing a TCF/LEF luciferase reporter gene, HEK 293 STF (ATCC, Manassas, VA, USA), treated with 10 mM LiCl and 10 mg/ml WNT3a, and normalized to protein concentration. For *Ctnnb1* sequencing cDNA was prepared from total RNA extracted from SCs-1, 2, 3. The region of *β-Catenin* (*Ctnnb1*) encoding exon 3 was sequenced and compared to WT. Primer sequences used were *Ctnnb1* Fw: 5′-CGC TGCGTGGACAATGGCTA-3′ and *Ctnnb1* Rv: 5′-CGTGTGGCAAGTTCCGCGTC-3′. Sequence alignment was performed using Ape software.

Mouse work

All mouse work was conducted in accordance with protocols approved by the Institutional Animal Care and Use Committee at the University of Miami. *Ptch1*$^{tm1Mps/J}$[66] and *B6.129S2-Trp53*$^{tm1Tyj/J}$[67] mice (Jackson laboratory, Bar Harbor, ME, USA) were mated to generate a breeding colony. Spontaneous tumors *Ptch1*$^{-/-}$;*Trp53*$^{+/+}$ or *Ptch1*$^{+/-}$;*Trp53*$^{+/-}$ were expanded and maintained in 6-week-old male *CD1-Foxn1*^{nu} mice as allografts (Charles River Laboratories, Worcester, MA, USA). For orthotopic studies, 100 000 viable cells were resuspended in 3 μl final volume and implanted into the cerebella of 6-week-old male *CD1-Foxn1*^{nu} mice using the stereotaxic coordinates 2 mm posterior to lambda, 2 mm lateral to the middle line and 2 mm deep. Treatment was started 2 days after implantation. The same coordinates and final volume were used to implant 10 000 viable cells for symptom-free

survival studies. For flank treatments, 1 000 000 viable cells were subcutaneously implanted into 6-week-old male *CD1-Foxn1^{nu}* mice and treatment started once the tumors reached a size of approximately 200 mm^3. Mouse tissues were fixed in formalin prior to be stained. For *in vivo* engraftment studies, the indicated numbers of viable cells from residual tumors were implanted into the flanks of 6-week-old male *CD1-Foxn1^{nu}* mice. For all *in vivo* studies, 50 μl of 50 mg/kg vismodegib (Selleckchem, Houston, TX, USA) or 10 mg/kg carnosate (Enzo, Farmingdale, NY, USA) both dissolved in dimethyl sulfoxide and were administrated daily via intra-peritoneal injection.

Statistical analysis

For *our ex vivo* analyses, the results shown represent the mean of at least three independent experiments ± s.e.m. For *in vivo* analyses, the results shown represent the mean and s.e.m. of at least six mice. For IHC quantification, the results shown represent the mean and s.e.m. of at least six fields from three different tumors. Sample sizes were chosen based on similar well-characterized experiments to ensure adequate power to detect a pre-specified effect size. Mice were randomly distributed to different treatments and the investigator blinded to the assignment until final tumor analyses. For symptom-free survival analysis, those mice that did not show tumors as per hematoxylin eosin staining 60 days after experiment initiation were excluded from the analyses. Significance in multiple group comparisons was determined using a one-way analysis of variance followed by a *post-hoc* Student–Newman–Keuls analysis. Two sample analyses were determined using a one-tailed Student's *t*-test. Data generated showed normal distribution with similar variances, and analysis was completed assuming equal variances. Statistical significance was reached when $P < 0.05$. The significance of tumor frequency was determined using a χ^2 test, and statistically significance determined when $\alpha < 0.05$. Survival significance was calculated using a Log-rank (Mantel–Cox) test and statistically significance reached when $P < 0.05$.

Supplementary Material

Refer to Web version on PubMed Central for supplementary material.

Acknowledgments

We would like to thank members of the Robbins, Capobianco and Pei laboratories for providing their insights during discussions regarding this manuscript. Also, we would like to acknowledge the skilled assistance of the Sylvester Cancer Center Flow Cytometry Core. *Funding*: Alex Lemonade Stand Foundation M1201547 (DJR), 1R21NS096502-01 (DJR), The University of Miami Women's Cancer Association (DJR), B*Cured 2016 (DJR), Childhood Brain Tumor Foundation (JR-B), FICYT POST10- 27 (JR-B), funds from the Sylvester Cancer Center (DJR), NIH R01GM081635 (EL), and R01GM103926 (EL).

References

1. Louis DN, Ohgaki H, Wiestler OD, Cavenee WK, Burger PC, Jouvet A, et al. The 2007 WHO classification of tumours of the central nervous system. Acta Neuropathol. 2007; 114:97–109. [PubMed: 17618441]
2. Crawford JR, MacDonald TJ, Packer RJ. Medulloblastoma in childhood: new biological advances. Lancet Neurol. 2007; 6:1073–1085. [PubMed: 18031705]

3. Gibson P, Tong Y, Robinson G, Thompson MC, Currle DS, Eden C, et al. Subtypes of medulloblastoma have distinct developmental origins. Nature. 2010; 468:1095–1099. [PubMed: 21150899]
4. Northcott, Pa, Dubuc, AM., Pfister, S., Taylor, MD. Molecular subgroups of medulloblastoma. Expert Rev Neurother. 2012; 12:871–884. [PubMed: 22853794]
5. Remke M, Ramaswamy V, Taylor MD. Medulloblastoma molecular dissection: the way toward targeted therapy. Curr Opin Oncol. 2013; 25:674–681. [PubMed: 24076581]
6. Olson JM. Therapeutic opportunities for medulloblastoma come of age. Cancer Cell. 2014; 25:267–269. [PubMed: 24651008]
7. Atwood SX, Whitson RJ, Oro AE. Advanced treatment for basal cell carcinomas. Cold Spring Harb Perspect Med. 2014; 4:a013581. [PubMed: 24985127]
8. Johnson RL, Rothman aL, Xie J, Goodrich LV, Bare JW, Bonifas JM, et al. Human homolog of patched, a candidate gene for the basal cell nevus syndrome. Science. 1996; 272:1668–1671. [PubMed: 8658145]
9. Aszterbaum M, Rothman a, Johnson RL, Fisher M, Xie J, Bonifas JM, et al. Identification of mutations in the human PATCHED gene in sporadic basal cell carcinomas and in patients with the basal cell nevus syndrome. J Invest Dermatol. 1998; 110:885–888. [PubMed: 9620294]
10. Ng JMY, Curran T. The Hedgehog's tale: developing strategies for targeting cancer. Nat Rev Cancer. 2011; 11:493–501. [PubMed: 21614026]
11. Rudin CM, Hann CL, Laterra J, Yauch RL, Callahan Ca, Fu L, et al. Treatment of medulloblastoma with hedgehog pathway inhibitor GDC-0449. N Engl J Med. 2009; 361:1173–1178. [PubMed: 19726761]
12. LoRusso PM, Rudin CM, Reddy JC, Tibes R, Weiss GJ, Borad MJ, et al. Phase I trial of hedgehog pathway inhibitor vismodegib (GDC-0449) in patients with refractory, locally advanced or metastatic solid tumors. Clin Cancer Res. 2011; 17:2502–2511. [PubMed: 21300762]
13. Robinson GW, Orr BA, Wu G, Gururangan S, Lin T, Qaddoumi I, et al. Vismodegib exerts targeted efficacy against recurrent sonic hedgehog-subgroup medulloblastoma: results from phase II Pediatric Brain Tumor Consortium Studies PBTC-025B and PBTC-032. J Clin Oncol. 2015; 33:2646–2654. [PubMed: 26169613]
14. Heppner GH. Tumor heterogeneity. Cancer Res. 1984; 44:2259–2265. [PubMed: 6372991]
15. Marusyk A, Polyak K. Tumor heterogeneity: causes and consequences. Biochim Biophys Acta. 2010; 1805:105–117. [PubMed: 19931353]
16. Boman BM, Wicha MS. Cancer stem cells: a step toward the cure. J Clin Oncol. 2008; 26:2795–2799. [PubMed: 18539956]
17. Dean M, Fojo T, Bates S. Tumour stem cells and drug resistance. Nat Rev Cancer. 2005; 5:275–284. [PubMed: 15803154]
18. Yauch RL, Dijkgraaf GJ, Alicke B, Januario T, Ahn CP, Holcomb T, et al. Smoothened mutation confers resistance to a Hedgehog pathway inhibitor in medulloblastoma. Science. 2009; 326:572–574. [PubMed: 19726788]
19. Wolfe CM, Green WH, Cognetta AB, Hatfield HK. Basal cell carcinoma rebound after cessation of vismodegib in a nevoid basal cell carcinoma syndrome patient. Dermatol Surg. 2012; 38:1863–1866. [PubMed: 22805146]
20. Sekulic A, Migden MR, Oro AE, Dirix L, Lewis KD, Hainsworth JD, et al. Efficacy and safety of vismodegib in advanced basal-cell carcinoma. N Engl J Med. 2012; 366:2171–2179. [PubMed: 22670903]
21. Tang JY, Mackay-Wiggan JM, Aszterbaum M, Yauch RL, Lindgren J, Chang K, et al. Inhibiting the hedgehog pathway in patients with the basal-cell nevus syndrome. N Engl J Med. 2012; 366:2180–2188. [PubMed: 22670904]
22. Meani RE, Lim S-W, Chang ALS, Kelly JW. Emergence of chemoresistance in a metastatic basal cell carcinoma patient after complete response to hedgehog pathway inhibitor vismodegib (GDC-0449). Australas J Dermatol. 2014; 55:218–221. [PubMed: 25117162]
23. Singh SK, Clarke ID, Terasaki M, Bonn VE, Hawkins C, Squire J, et al. Identification of a cancer stem cell in human brain tumors. Cancer Res. 2003; 63:5821–5828. [PubMed: 14522905]

24. Singh SK, Hawkins C, Clarke ID, Squire JA, Bayani J, Hide T, et al. Identification of human brain tumour initiating cells. Nature. 2004; 432:396–401. [PubMed: 15549107]
25. Ward RJ, Lee L, Graham K, Satkunendran T, Yoshikawa K, Ling E, et al. Multipotent CD15+ cancer stem cells in Patched-1—deficient mouse medulloblastoma. Cancer Res. 2009:4682–4690. [PubMed: 19487286]
26. Read T-A, Fogarty MP, Markant SL, McLendon RE, Wei Z, Ellison DW, et al. Identification of CD15 as a marker for tumor-propagating cells in a mouse model of medulloblastoma. Cancer Cell. 2009; 15:135–147. [PubMed: 19185848]
27. Corno D, Pala M, Cominelli M, Cipelletti B, Leto K, Croci L, et al. Gene signatures associated with mouse postnatal hindbrain neural stem cells and medulloblastoma cancer stem cells identify novel molecular mediators and predict human medulloblastoma molecular classification. Cancer Discov. 2012; 2:554–568. [PubMed: 22628409]
28. Vanner RJ, Remke M, Gallo M, Selvadurai HJ, Coutinho F, Lee L, et al. Quiescent sox2(+) cells drive hierarchical growth and relapse in sonic hedgehog subgroup medulloblastoma. Cancer Cell. 2014; 26:33–47. [PubMed: 24954133]
29. Ahlfeld J, Favaro R, Pagella P, Kretzschmar HA, Nicolis S, Schüller U. Sox2 requirement in sonic hedgehog-associated medulloblastoma. Cancer Res. 2013; 73:3796–3807. [PubMed: 23596255]
30. Huang X, Ketova T, Litingtung Y, Chiang C. Isolation, enrichment, and maintenance of medulloblastoma stem cells. J Vis Exp. 2010; 43:2086.
31. Nusse R. Wnt signaling and stem cell control. Cell Res. 2008; 18:523–527. [PubMed: 18392048]
32. Koch A, Waha A, Tonn JC, Sörensen N, Berthold F, Wolter M, et al. Somatic mutations of WNT/wingless signaling pathway components in primitive neuroectodermal tumors. Int J Cancer. 2001; 93:445–449. [PubMed: 11433413]
33. Thompson MC, Fuller C, Hogg TL, Dalton J, Finkelstein D, Lau CC, et al. Genomics identifies medulloblastoma subgroups that are enriched for specific genetic alterations. J Clin Oncol. 2006; 24:1924–1931. [PubMed: 16567768]
34. Kemler R. From cadherins to catenins: cytoplasmic protein interactions and regulation of cell adhesion. Trends Genet. 1993; 9:317–321. [PubMed: 8236461]
35. Waterman ML. Lymphoid enhancer factor/T cell factor expression in colorectal cancer. Cancer Metastasis Rev. 2004; 23:41–52. [PubMed: 15000148]
36. Lewis SL, Khoo P-L, De Young RA, Steiner K, Wilcock C, Mukhopadhyay M, et al. Dkk1 and Wnt3 interact to control head morphogenesis in the mouse. Development. 2008; 135:1791–1801. [PubMed: 18403408]
37. Klein PS, Melton DA. A molecular mechanism for the effect of lithium on development. Proc Natl Acad Sci USA. 1996; 93:8455–8459. [PubMed: 8710892]
38. Liu J, Pan S, Hsieh MH, Ng N, Sun F, Wang T, et al. Targeting Wnt-driven cancer through the inhibition of Porcupine by LGK974. Proc Natl Acad Sci USA. 2013; 110:20224–20229. [PubMed: 24277854]
39. de la Roche M, Rutherford TJ, Gupta D, Veprintsev DB, Saxty B, Freund SM, et al. An intrinsically labile α-helix abutting the BCL9-binding site of β-catenin is required for its inhibition by carnosic acid. Nat Commun. 2012; 3:680. [PubMed: 22353711]
40. Ewan K, Pajak B, Stubbs M, Todd H, Barbeau O, Quevedo C, et al. A useful approach to identify novel small-molecule inhibitors of Wnt-dependent transcription. Cancer Res. 2010; 70:5963–5973. [PubMed: 20610623]
41. Eguchi M, Nguyen C, Lee SC, Kahn M. ICG-001, a novel small molecule regulator of TCF/beta-catenin transcription. Med Chem. 2005; 1:467–472. [PubMed: 16787331]
42. Gandhirajan RK, Staib PA, Minke K, Gehrke I, Plickert G, Schlösser A, et al. Small molecule inhibitors of Wnt/beta-catenin/lef-1 signaling induces apoptosis in chronic lymphocytic leukemia cells in vitro and in vivo. Neoplasia. 2010; 12:326–335. [PubMed: 20360943]
43. Anne SL, Govek E-E, Ayrault O, Kim JH, Zhu X, Murphy DA, et al. WNT3 inhibits cerebellar granule neuron progenitor proliferation and medulloblastoma formation via MAPK activation. PLoS ONE. 2013; 8:e81769. [PubMed: 24303070]

44. Zinke J, Schneider FT, Harter PN, Thom S, Ziegler N, Toftgård R, et al. β-Catenin-Gli1 interaction regulates proliferation and tumor growth in medulloblastoma. Mol Cancer. 2015; 14:17. [PubMed: 25645196]
45. Pöschl J, Bartels M, Ohli J, Bianchi E, Kuteykin-Teplyakov K, Grammel D, et al. Wnt/β-catenin signaling inhibits the Shh pathway and impairs tumor growth in Shh-dependent medulloblastoma. Acta Neuropathol. 2014; 127:605–607. [PubMed: 24531885]
46. Azad N, Rasoolijazi H, Joghataie MT, Soleimani S. Neuroprotective effects of carnosic Acid in an experimental model of Alzheimer's disease in rats. Cell J. 2011; 13:39–44. [PubMed: 23671826]
47. Piccin D, Morshead CM. Wnt signaling regulates symmetry of division of neural stem cells in the adult brain and in response to injury. Stem Cells. 2011; 29:528–538. [PubMed: 21425415]
48. Lange C, Mix E, Rateitschak K, Rolfs A. Wnt signal pathways and neural stem cell differentiation. Neurodegener Dis. 2006; 3:76–86. [PubMed: 16909041]
49. Fan X, Eberhart CG. Medulloblastoma stem cells. J Clin Oncol. 2008; 26:2821–2827. [PubMed: 18539960]
50. Zhao X, Ponomaryov T, Ornell KJ, Zhou P, Dabral SK, Pak E, et al. RAS/MAPK activation drives resistance to smo inhibition, metastasis, and tumor evolution in Shh pathway-dependent tumors. Cancer Res. 2015; 75:3623–3635. [PubMed: 26130651]
51. Cha YH, Kim NH, Park C, Lee I, Kim HS, Yook JI. MiRNA-34 intrinsically links p53 tumor suppressor and Wnt signaling. Cell Cycle. 2012; 11:1273–1281. [PubMed: 22421157]
52. Kim NH, Kim HS, Kim N-G, Lee I, Choi H-S, Li X-Y, et al. p53 and miRNA-34 are Suppressors of Canonical Wnt Signaling. Sci Signal. 2011; 4:ra71. [PubMed: 22045851]
53. Voorneveld PW, Kodach LL, Jacobs RJ, van Noesel CJM, Peppelenbosch MP, Korkmaz KS, et al. The BMP pathway either enhances or inhibits the Wnt pathway depending on the SMAD4 and p53 status in CRC. Br J Cancer. 2015; 112:122–130. [PubMed: 25393365]
54. Zhukova N, Ramaswamy V, Remke M, Pfaff E, Shih DJH, Martin DC, et al. Subgroup-specific prognostic implications of TP53 mutation in medulloblastoma. J Clin Oncol. 2013; 31:2927–2935. [PubMed: 23835706]
55. Tabori U, Baskin B, Shago M, Alon N, Taylor MD, Ray PN, et al. Universal poor survival in children with medulloblastoma harboring somatic TP53 mutations. J Clin Oncol. 2010; 28:1345–1350. [PubMed: 20142599]
56. Kool M, Jones DTW, Jäger N, Northcott PA, Pugh TJ, Hovestadt V, et al. Genome sequencing of SHH medulloblastoma predicts genotype-related response to smoothened inhibition. Cancer Cell. 2014; 25:393–405. [PubMed: 24651015]
57. Yang SH, Andl T, Grachtchouk V, Wang A, Liu J, Syu L-J, et al. Pathological responses to oncogenic Hedgehog signaling in skin are dependent on canonical Wnt/beta3-catenin signaling. Nat Genet. 2008; 40:1130–1135. [PubMed: 19165927]
58. Youssef KK, Lapouge G, Bouvrée K, Rorive S, Brohée S, Appelstein O, et al. Adult interfollicular tumour-initiating cells are reprogrammed into an embryonic hair follicle progenitor-like fate during basal cell carcinoma initiation. Nat Cell Biol. 2012; 14:1282–1294. [PubMed: 23178882]
59. Tam WL, Ng HH. Sox2: masterminding the root of cancer. Cancer Cell. 2014; 26:3–5. [PubMed: 25026204]
60. Kenney AM, Rowitch DH. Sonic hedgehog promotes G1 cyclin expression and sustained cell cycle progression in mammalian neuronal precursors. Mol Cell Biol. 2000; 20:9055–9067. [PubMed: 11074003]
61. Lee HY, Greene LA, Mason CA, Manzini MC. Isolation and culture of post-natal mouse cerebellar granule neuron progenitor cells and neurons. J Vis Exp. 2009; 23:990.
62. Gritti A, Parati E, Cova L, Frolichsthal P, Galli R, Wanke E, et al. Multipotential stem cells from the adult mouse brain proliferate and self-renew in response to basic fibroblast growth factor. J Neurosci. 1996; 16:1091–1100. [PubMed: 8558238]
63. Kennedy MWL, Kao KR. Xrel3/XrelA attenuates β-catenin-mediated transcription during mesoderm formation in Xenopus embryos. Biochem J. 2011; 435:247–257. [PubMed: 21214516]
64. Rodriguez-Blanco J, Martín V, Herrera F, García-Santos G, Antolín I, Rodriguez C. Intracellular signaling pathways involved in post-mitotic dopaminergic PC12 cell death induced by 6-hydroxydopamine. J Neurochem. 2008; 107:127–140. [PubMed: 18665912]

65. Fei DL, Li H, Kozul CD, Black KE, Singh S, Gosse JA, et al. Activation of Hedgehog signaling by the environmental toxicant arsenic may contribute to the etiology of arsenic-induced tumors. Cancer Res. 2010; 70:1981–1988. [PubMed: 20179202]

66. Goodrich LV, Milenković L, Higgins KM, Scott MP. Altered neural cell fates and medulloblastoma in mouse patched mutants. Science. 1997; 277:1109–1113. [PubMed: 9262482]

67. Wetmore C, Eberhart DE, Curran T. Loss of p53 but not ARF accelerates medulloblastoma in mice heterozygous for patched. Cancer Res. 2001; 61:513–516. [PubMed: 11212243]

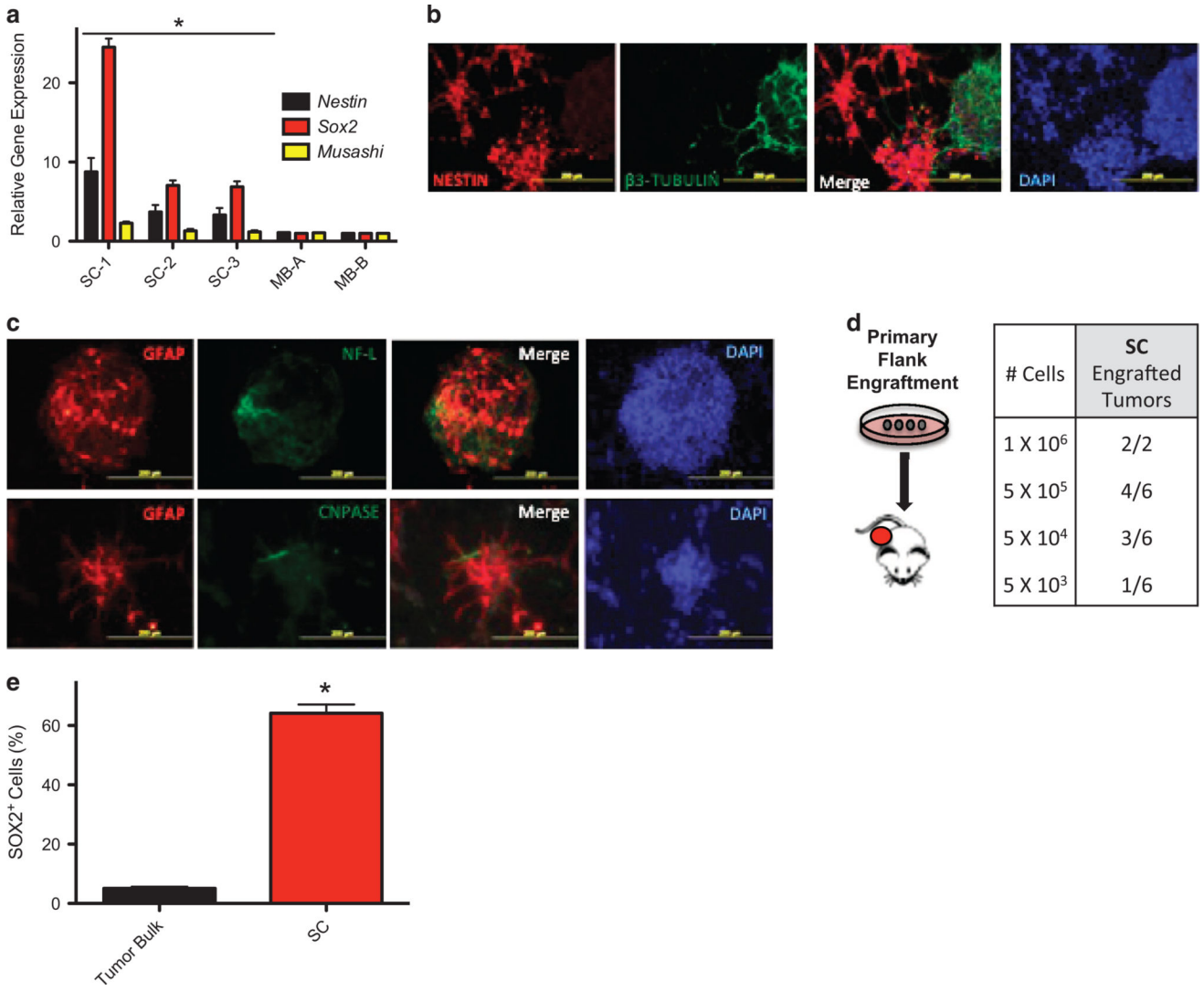

Figure 1.

Medulloblastoma sphere cultures display stem cell properties. (**a**) The expression of the indicated progenitor cell biomarkers, from three independently derived *Trp53*-deficient MB sphere cultures (SC-1, 2 and 3) and two primary MBs (MB-A and MB-B), was determined and then normalized to that of MB-A. (**b**) SCs were immunostained for neuronal progenitor biomarkers (NESTIN and β3-TUBULIN). (**c**) The level of SC pluripotency was determined by examining the biomarkers GLIAL FRIBRILLARY ACIDIC PROTEIN (GFAP), NEUROFILAMENT-LARGE (NF-L) or CYCLIC-NUCLEOTIDE-PHOSPHODIESTERASE (CNPASE). Representative images of immunostained SC-2 are shown. (**d**) The indicated numbers of viable SC-2 cells were implanted subcutaneously into the flanks of immunocompromised mice. The frequency and number of tumor engraftments is shown. (**e**) The percentage of $SOX2^+$ cells in MB flank tumors and SCs was determined by FACS analysis.

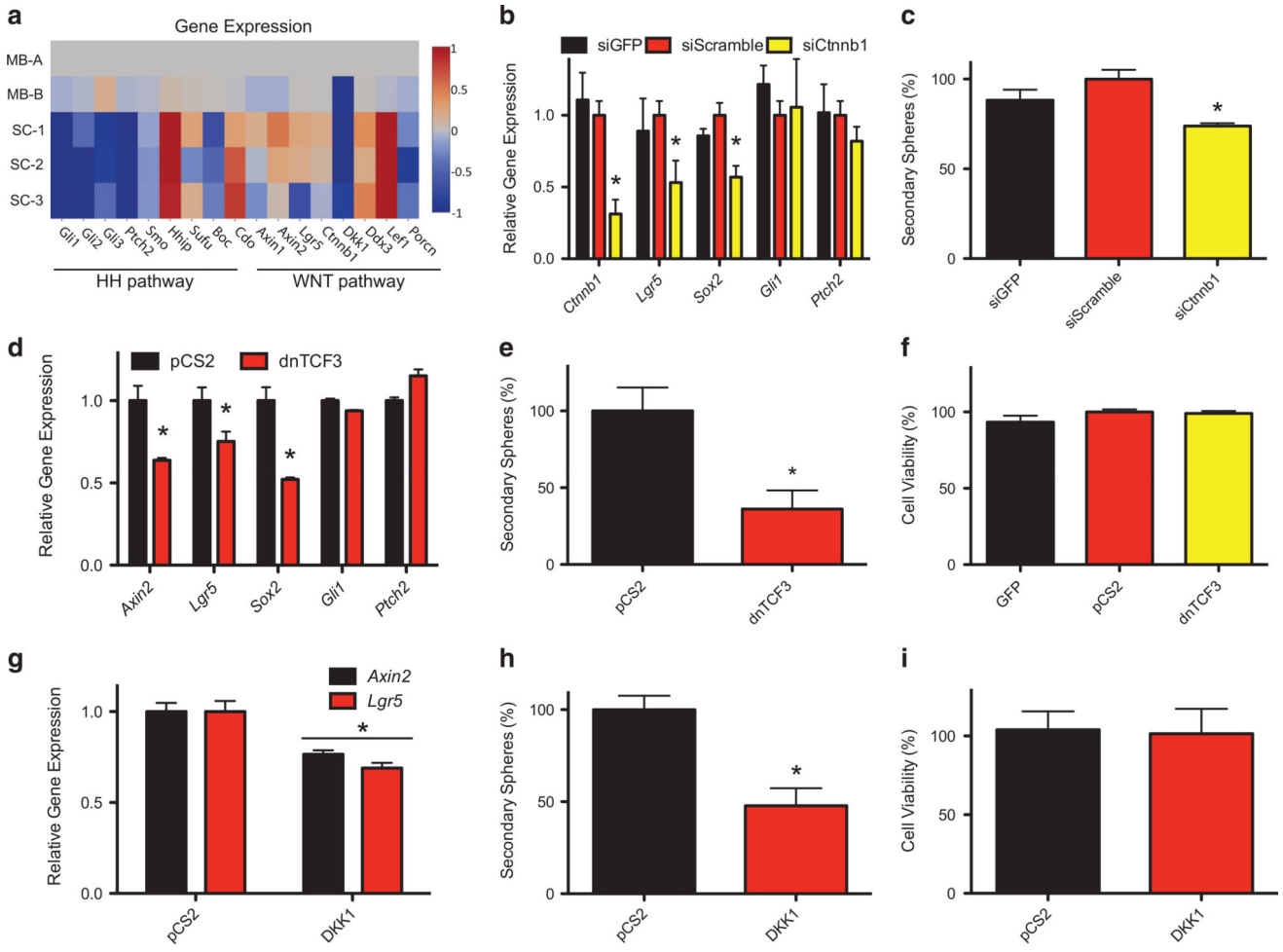

Figure 2.

The self-renewal of medulloblastoma sphere cultures is dependent on WNT activity. (**a**) A heat map representing the relative gene expression of SHH (*Gli1*, *Gli2*, *Gli3*, *Ptch2*, *Smo, Hhip, Sufu, Boc, Cdo*) and WNT pathway-related genes (*Axin1*, *Axin2*, *Lgr5*, *Ctnnb1, Dkk1, Ddx3, Lef1, Porcn*), as determined in the indicated *Trp53*-deficient SCs and *Trp53*-deficient MB tissues (MB-A and MB-B). The color scale was calculated using Log2 transformed gene expression data normalized to their expression in MB-A. (**b**) SC-2 were transfected with the indicated siRNA smart pools, and the expression of the indicated genes determined 72 h later. (**c**) The ability of SC-2 to form secondary spheres 72 h after transfection with the indicated siRNA smart pool was determined. (**d**) SC-2 were transfected with a plasmid expressing a *dnTCF3* construct or a control plasmid (*pCS2*), and the expression of the indicated genes determined 48 h later. (**e**) The ability of SC-2 to form secondary spheres was determined 48 h after transfection with a *dnTCF3* expression plasmid or control plasmid (*pCS2*). (**f**) SC-2 was transfected with a plasmid expressing a *dnTCF3* construct or control plasmid (*pCS2*) and cell viability determined 5 days later using an MTT reduction assay. (**g**) SC-2 was transfected with a plasmid expressing *DKK1* or control plasmid (*pCS2*) and the expression of WNT target genes determined. (**h**) The ability of SC-2 to form secondary spheres was determined 48 h after transfection with a plasmid expressing

DKK1 or control plasmid (*pCS2*). (**i**) SC-2 was transfected with a plasmid expressing *DKK1* or control plasmid (*pCS2*) and cell viability determined 5 days later using an MTT reduction assay. Results were normalized to that from *pCS2* transfected cultures unless otherwise indicated. MTT, 3-(4,5-dimethyl-2-thiazolyl) 2,5-diphenyl-2H-tetrazolium bromide.

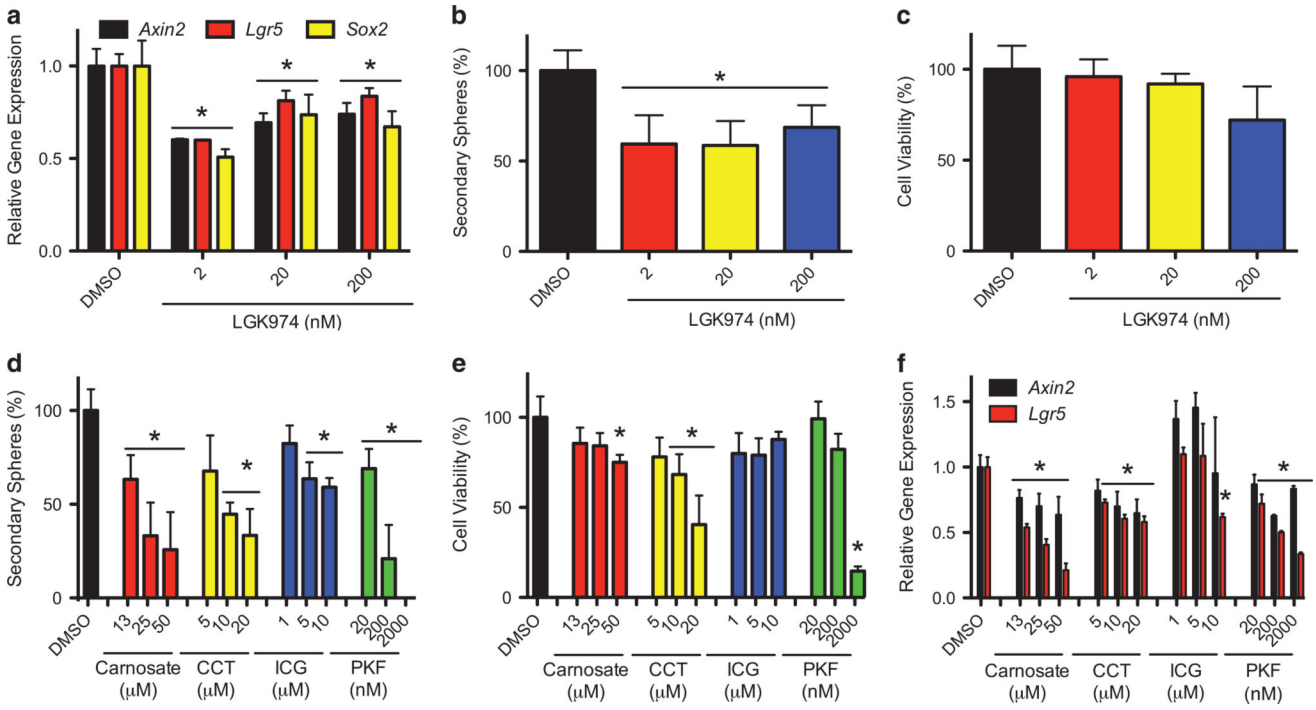

Figure 3.

Small-molecule WNT inhibitors attenuate the self-renewal of medulloblastoma sphere cultures. (**a**) SC-2 were treated with the indicated concentrations of the PORCUPINE inhibitor LGK974, and the expression of the indicated genes determined 72 h later. (**b**) The ability of SC-2 to form secondary spheres was determined following incubation (72 h) with the indicated concentrations of LGK974. (**c**) SC-2 were incubated with the indicated concentrations of LGK974, and cell viability determined 5 days later using an MTT reduction assay. (**d**) The ability of SC-2 to form secondary spheres was determined following incubation (24 h) with the indicated concentrations of TCF/β-CATENIN inhibitors (carnosate, CCT-031374 hydrobromide [CCT], ICG-001 [ICG] or PKF-115-584 [PKF]). (**e**) SC-2 were incubated for 72 h with the indicated concentrations of TCF/β-CATENIN inhibitors, and cell viability determined 5 days later using an MTT reduction assay. (**f**) SC-2 were treated with the indicated TCF/β-CATENIN inhibitors for 24 h. The expression of the indicated genes was determined. Results were normalized to dimethyl sulfoxide control. MTT, 3-(4,5-dimethyl-2-thiazolyl) 2,5-diphenyl-2H-tetrazolium bromide.

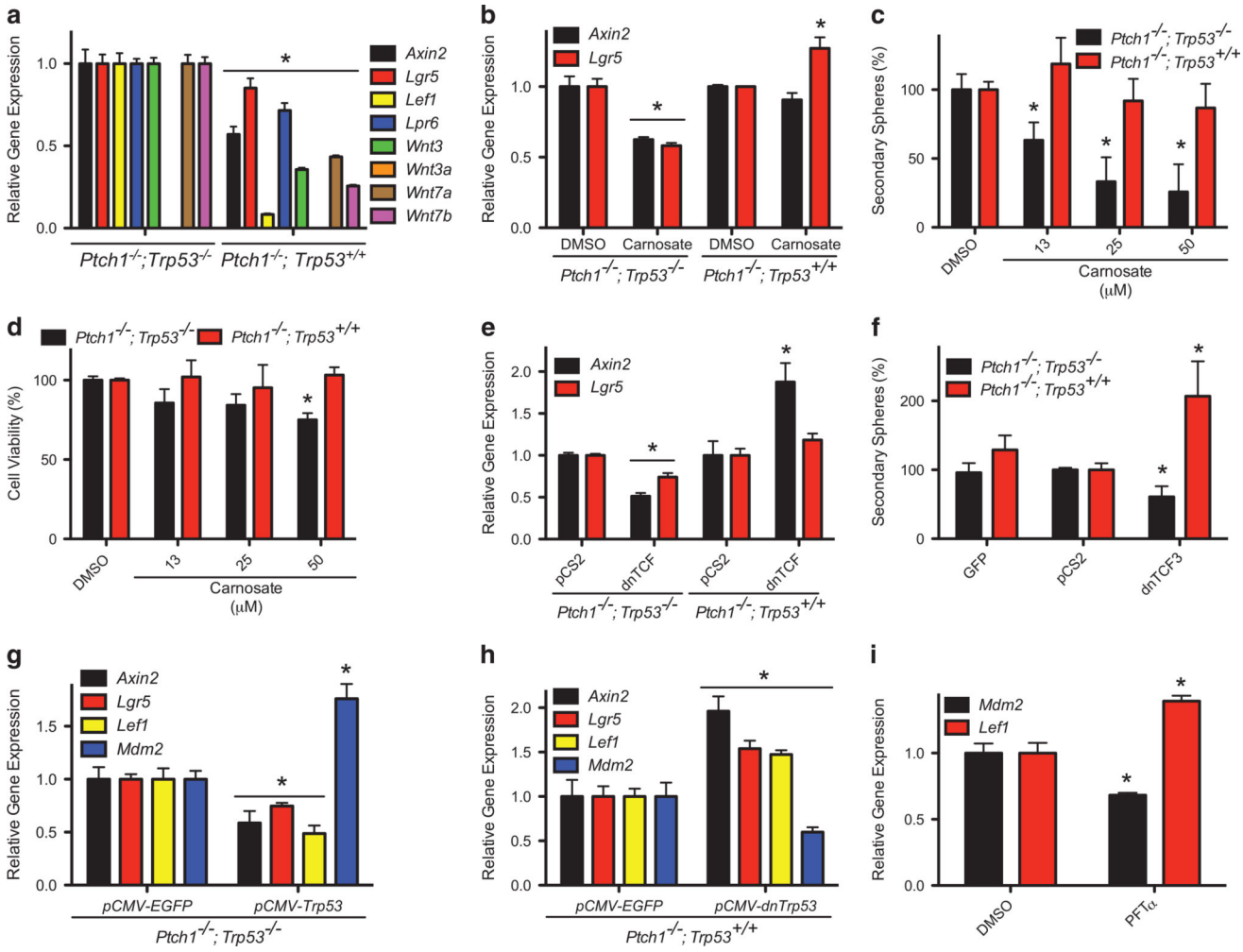

Figure 4.

MPC enriched cultures expressing wild-type *Trp53* are not WNT-dependent. (**a**) The expression of the indicated genes was determined in *Ptch1*$^{-/-}$;*Trp53*$^{-/-}$ or *Ptch1*$^{-/-}$;*Trp53*$^{+/+}$ SCs, and normalized to the data from *Ptch1*$^{-/-}$;*Trp53*$^{-/-}$ cultures. (**b**) SC cultures were treated with 25 μM carnosate for 24 h, and the expression of the indicated WNT target genes determined. (**c**) The ability of the SCs to form secondary spheres, following incubation (24 h) with the indicated concentrations of carnosate, was determined. (**d**) The indicated SCs were incubated for 3 days with the various concentrations of carnosate, and cell viability determined 5 days later using an MTT reduction assay. The results were normalized to those from the dimethyl sulfoxide control. (**e**) SCs were transfected with a plasmid expressing a *dnTCF3* construct or a control plasmid (*pCS2*), and the expression of the indicated WNT target genes determined 48 h later. (**f**) The ability of SCs to form secondary spheres was determined 48 h after transfection with plasmids expressing *dnTCF3*, a control plasmid (*pCS2*) or *GFP*. Results were normalized to those from the *pCS2* control. (**g**) *Ptch1*−/−;*Trp53*$^{-/-}$ SCs were transfected with plasmids expressing wild-type P53 (*pCMV-Trp53*), or an enhanced green fluorescent protein (EGFP) (*pCMV-EGFP*) control vector, and the expression of the indicated genes determined 72 h later. (**h**) *Ptch1*$^{-/-}$; *Trp53*$^{+/+}$ SCs were

transfected with plasmids expressing dominant negative P53 (*pCMV-dnTrp53*) or EGFP (*pCMV-EGFP*), and the expression of the indicated genes determined 72 h later. The results were normalized to those from the EGFP expressing cultures. (**i**) *Ptch1*$^{-/-}$;*Trp53*$^{+/+}$ SCs were incubated with the P53/MDM2 inhibitor Pifithrin-α (PFT-α) for 24 h, and the expression of the indicated genes determined. The results were normalized to those from the dimethyl sulfoxide control. MTT, 3-(4,5-dimethyl-2-thiazolyl) 2,5-diphenyl-2H-tetrazolium bromide.

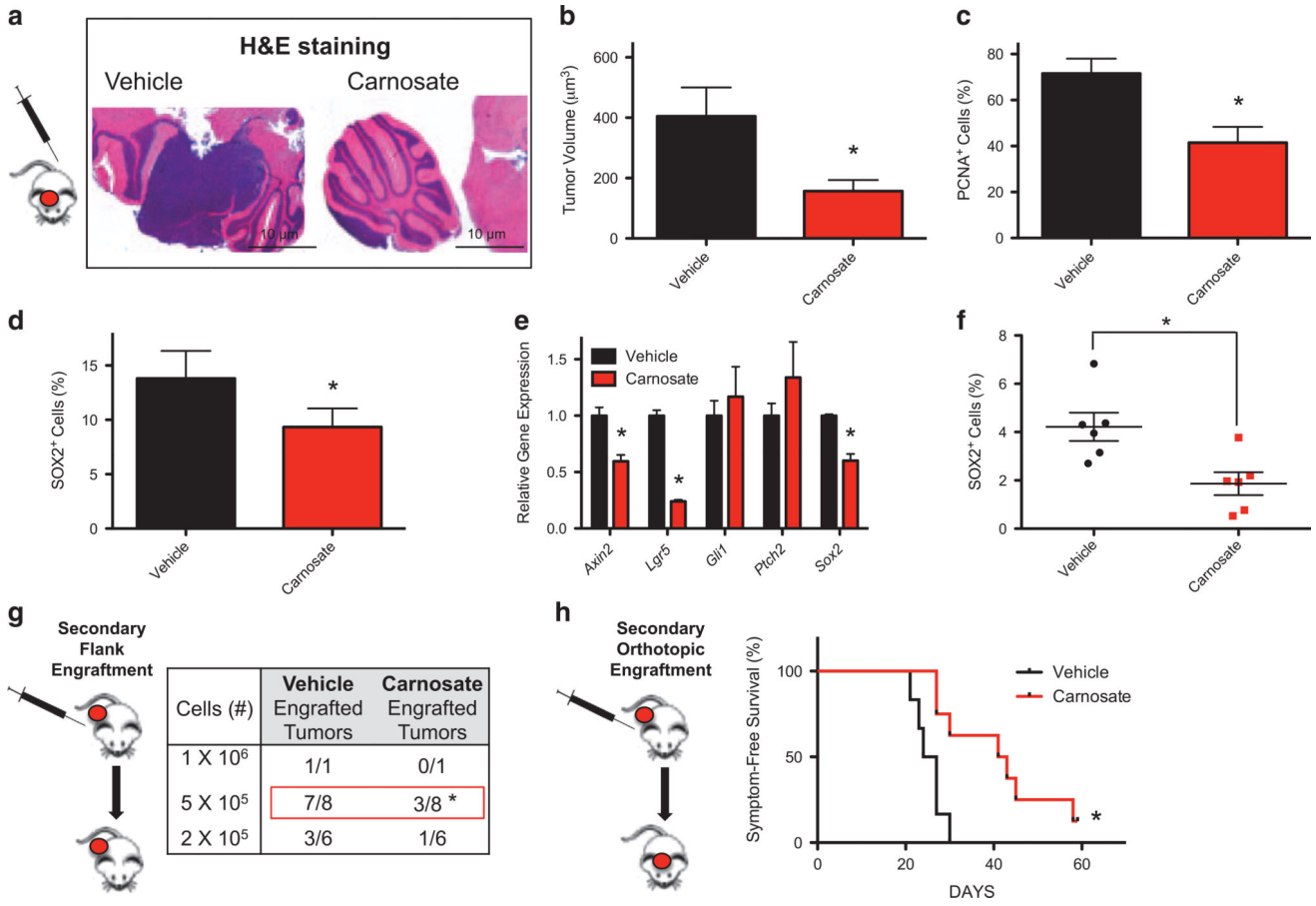

Cells (#)	Vehicle Engrafted Tumors	Carnosate Engrafted Tumors
1 X 10^6	1/1	0/1
5 X 10^5	7/8	3/8 *
2 X 10^5	3/6	1/6

Figure 5.

The propagation and growth of *Trp53*-deficient, SHH-subgroup medulloblastoma is WNT-dependent. *Trp53* mutant, *Ptch1*-driven MB tissue, which had never been cultured *ex vivo*, was orthotopically implanted into the cerebellum of immunocompromised mice. These mice were then treated with carnosate or vehicle for 20 days, or until they developed MB symptoms. The mice were then killed and their brains collected. (**a**) Representative hematoxylin eosin staining of orthotopic MB tissue from a carnosate or vehicle-treated mouse is shown. (**b**) The volume of residual orthotopic tumors from these mice was calculated, and the mean volume and s.e.m. shown. (**c**) The residual orthotopic tumors from these mice were immunostained for the proliferation biomarker PCNA, and the numbers of $PCNA^+$ cells quantified and normalized to total cell number per field (%). (**d**) The residual orthotopic tumors from these mice were immunostained for the MPC biomarker SOX2, and the numbers of $SOX2^+$ cells quantified and normalized to total cell number per field (%). (**e**) MB tumor tissue was subcutaneously implanted into the flanks of immunocompromised mice, and treated daily with of carnosate, or vehicle control, for 8 days. The expression of the indicated genes in residual flank tumors was then determined. (**f**) The enrichment of $SOX2^+$ cells in residual flank tissue, from carnosate or vehicle-treated mice, was determined by FACS analysis. (**g**) The indicated number of viable cells from residual MB tissue was transplanted into additional immunocompromised mice, and the frequency of tumor engraftment determined. (**h**) Equal numbers of viable cells from residual flank MB tissue

were implanted into the cerebellum of additional immunocompromised mice, and MB symptom-free survival monitored for 60 days. Results were normalized to vehicle control.